ECE 435 CS-MRI Report

Alexander Faust

December 2023

Abstract

In this final project the objective is the use the theory of convex optimization to perform compressed sensing on MRI data sets. Unlike Nyquist, compressed sensing theory states that the number of samples are determined by how "predictable" the signal is. Nyquist predicts number of samples determined by bandwidth. For compressed sensing three different priors are assumed: the signal 1. approximately piecewise constant (i.e. extremely high frequency), 2. approximately piecewise linear, or 3. "sparse" in some domain. The motivation here is that by developing an orthonormal basis (o.n.b) out of wavelets we can have very few nonzero components in the image reconstruction - more or less the sparsity condition. And resulting from this motivates the idea of utilizing compressed sensing in order to beat the Nyquist sampling theorem and perform image reconstruction on massive MRI data sets at a faster rate. The source of the data used in this experiment can be found here: https://openneuro.org/datasets/ds001499/versions/1.3.0 and we will be examining anatomical recordings (MRI) for patients CSI1 through CSI4 considering T1 and T2 weighting.

1 Navigating the Images

As a guiding exercise, it will be useful to show the sagittal, coronal, and axial cross-sections of the data sets. What is immediately apparent are the different grayscale color regions in the image; the brightness of which each depend on the T1 and T2 times. T1-weighted imaging yield brighter regions for **shorter** times. T2-weighted imaging yield brighter regions for **longer** times.

Structure	T1 [ms]	T2 [ms]
White Matter	510	67
Grey Matter	760	77
Cerebrospinal Fluid	2650	280

Figure 1. Times Through Structures

According to Figure 1. we can classify the three main greyscale regions within the different MRI images shown in Figure 2. to its corresponding structural region. Thus, for the T1-weighted imaging in Figure 2. the brightest of spots correspond to regions of white matter, in-between areas are grey matter, and then the darkest are cerebrospinal fluid zones. And since that is the case for T1-weighted imaging, then the opposite will be true for the T2-weighted images. Therefore, the brightest spots in the T2-weighted imaging are cerbrospinal fluid regions, in-between are once again grey matter, and the darkest are white matter zones.

Inversion Time

The next preliminary area of study concerns the inversion times for T1 and T2-weighted imaging, found within the json files provided by OpenNeuro. Inversion times can be described as the time between the 180° inversion pulse and the time of excitation pulse activation. With respect to the relevance of inversion time to weighting, there is a significant relevance in T1-weighted imaging. In particular, the inversion time can serve as an indicator regarding how much T1 recovery occurs before signal measure. In NMR theory this corresponds to how much longitudinal

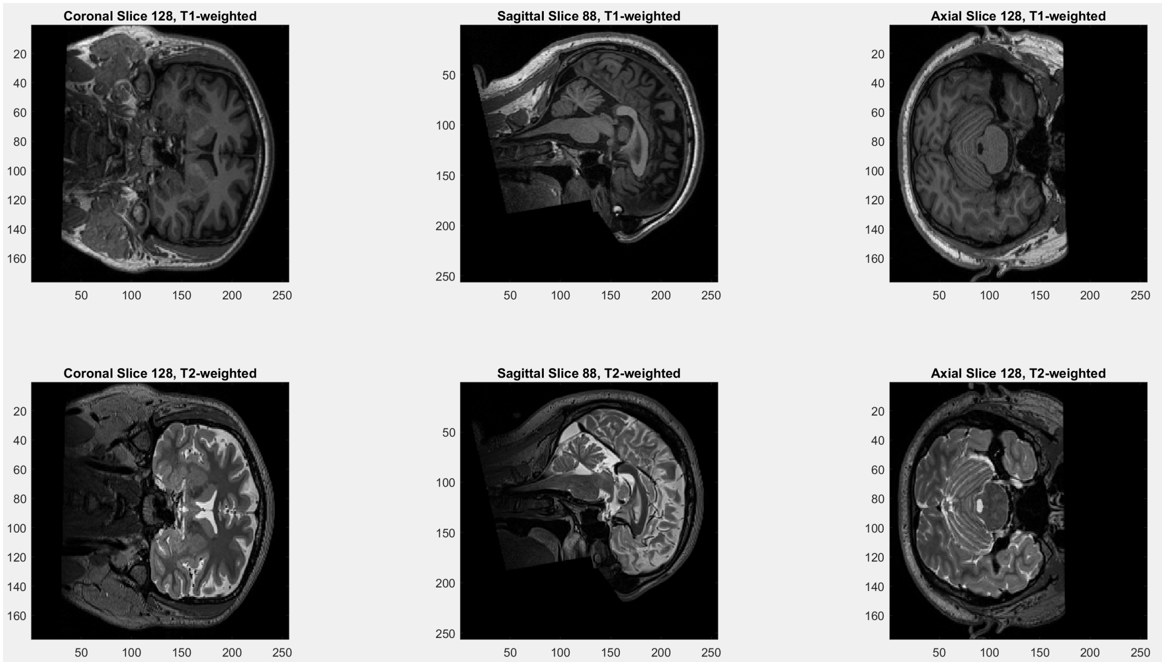

Figure 2. Sample Images Subplot at Different Slices

magnetization is provided before the measurement. With all this being said, an inversion time of 0.9 seconds (as was given in by OpenNeuro for these tests) was enough to maximize contrast between different tissues. One again, upon inspection of the images in Figure 2, it is clear that there is a strong contrast between these structures.

Echo Time

As far as how echo times relate to different weighting schemes, we first define echo time as the time between the excitation pulse and the echo signal peak. With echo times we are more concerned with the transient, random dephasing behavior. Thus, for longer echo times we can get a better understanding of the random dephasing that occurs which implies that we obtain better T2 contrast. An echo time of 1.97ms was taken for the provided images which I would assume is a relatively short time in the grand scheme of things. This would yield better T1 contrast as a result.

Repetition Time

Finally, we should examine the repetition time in this experiment. The time between a sequence of two pulse sequences to the same slice is quantified as the repetition time. This effects both T1 and T2-weighting in opposite ways. For long repetition times T1 weighting is reduced but increases T2 weighting, whereas short repetition times enhance T1 contrast alone. This can be interpreted in NMR such that preserving magnetic resonance/precession with increasing repetition times will yield a greater "resolution", if you will, of the transient behavior quantified by T2. This simply leads to better T2 contrast. A repetition time of 2.3 seconds was given for the captures which corresponds to a reduction in T1 weighting but a greater T2-weighting.

Before continuing, in order for our experiments to have meaningful results it should be noted that I am choosing to use slices near the center of the volume in order to determine the success or failure of each method.

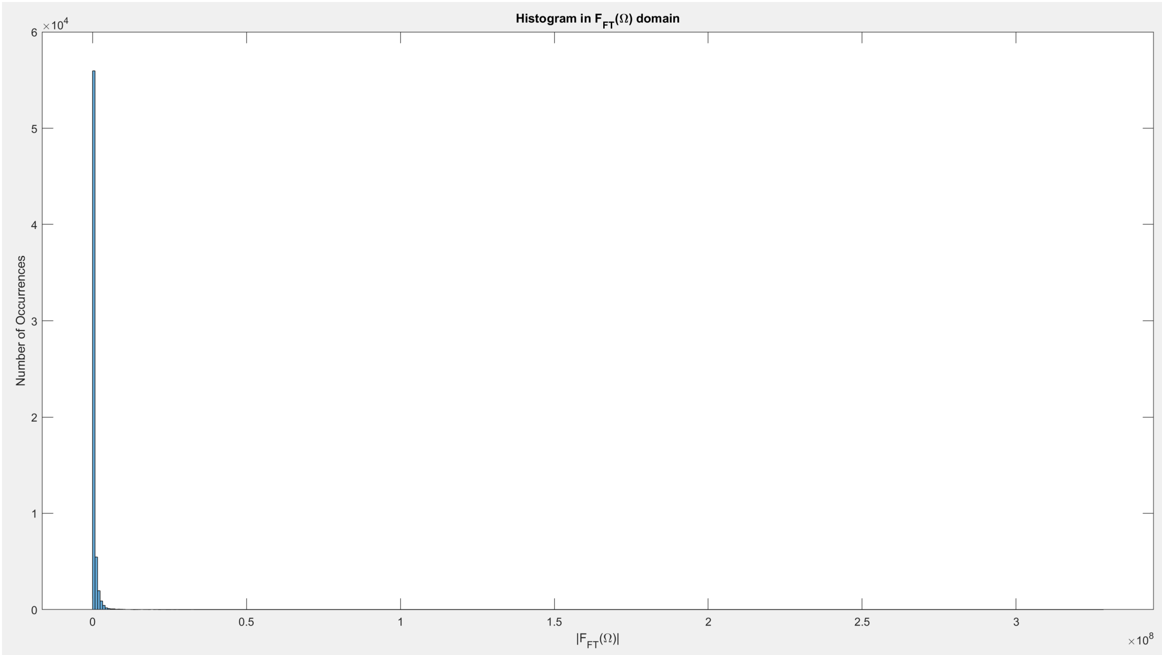

Figure 3. Histogram of magnitude of guiding image

2 Compression in Fourier Domain

To begin, the scaled magnitude image of our chosen guiding image will be displayed in the Fourier domain as motivation. Referring to Figure 3. we can see that there exists sparsity in the Fourier domain due to several low magnitude terms! Note that the displayed histogram was chosen to contain N = 400 bins. What can also be observed is the presence of very few high magnitude coefficients because of the extension of the x-axis in the histogram. These coefficients contain the important information in the guiding image.

Now that we know our guiding image is sparse in the Fourier domain we can reconstruct our guiding image with fewer coefficients since we can effectively zero out a large percentage of these low magnitude coefficients. And thus, we can rest assured knowing that we won't lose a significant portion of the information bearing signal through compression. Lastly, examining the 2D magnitude spectrum of the guiding image we can once

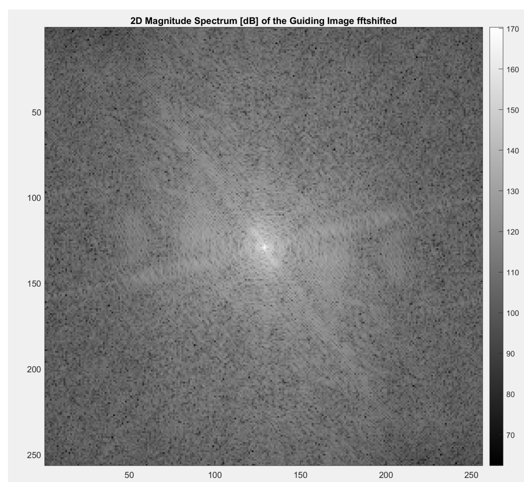

Figure 4. 2-D Magnitude Spectrum

again see the presence of sparsity. With all of this in mind we can begin comparing the ground truth (guiding image) to the reconstructed image.

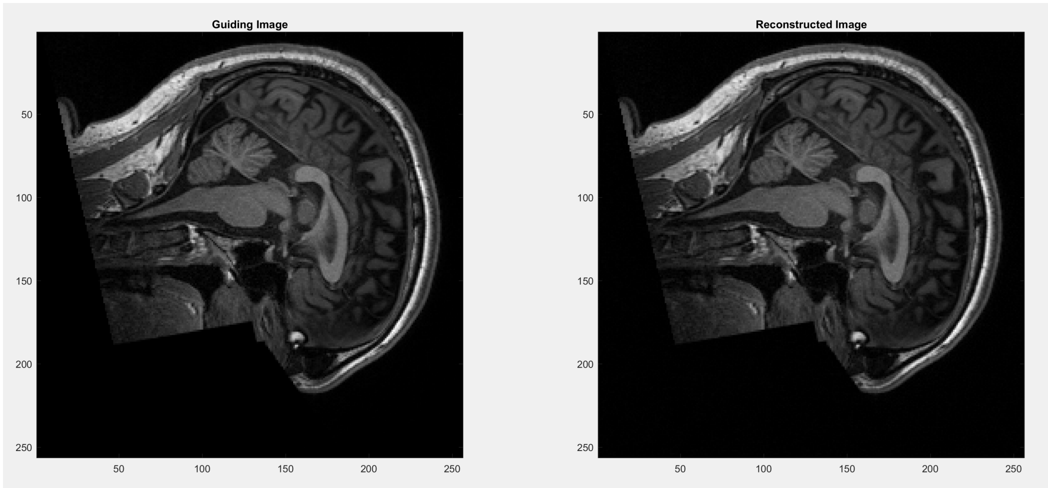

30% Compression with MSE = 51,258.39

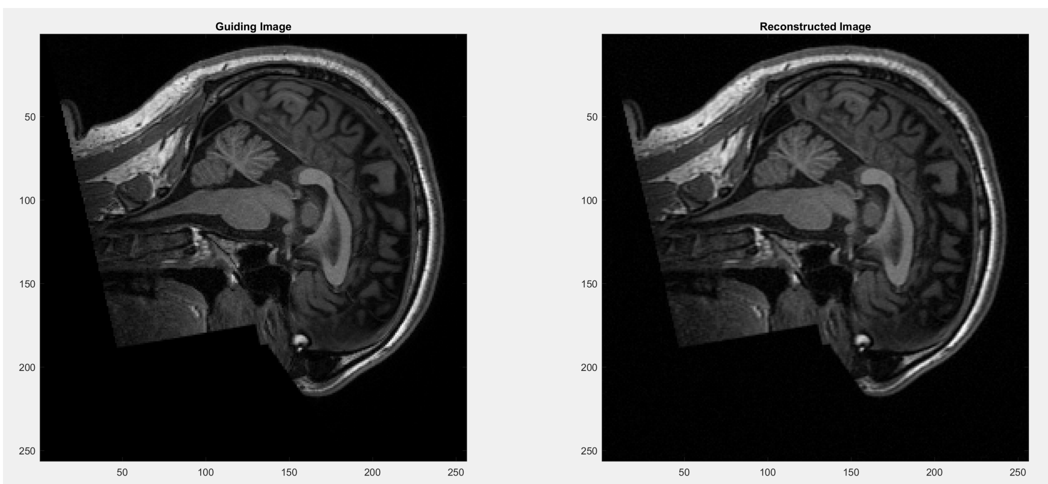

60% Compression with MSE = 306,383.2545

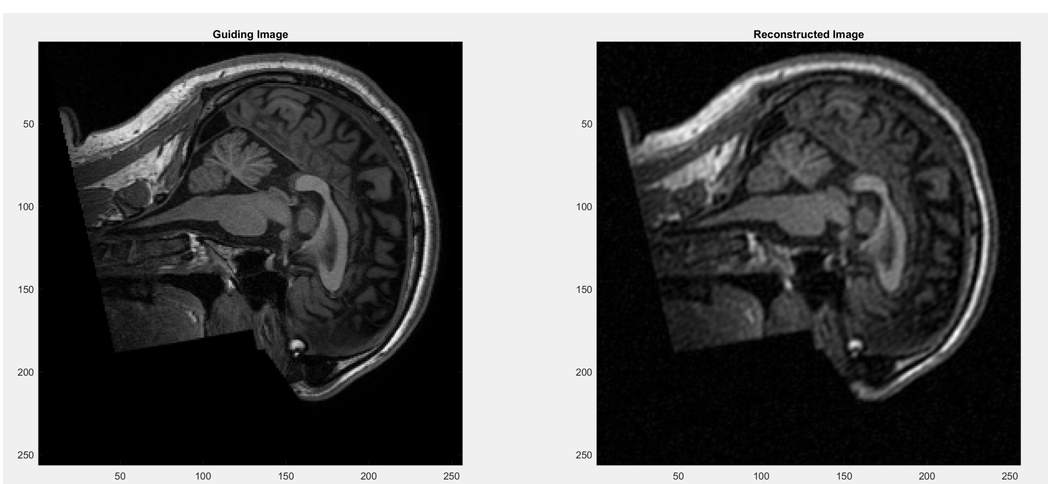

90% Compression with MSE = 1,972,412.6191

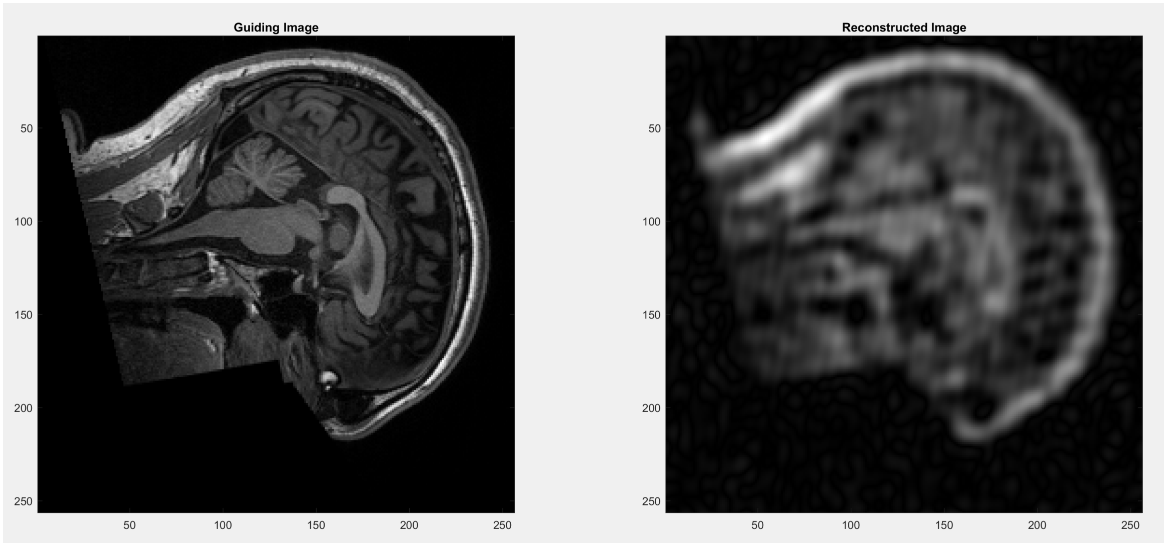

99% Compression with MSE = 8,636,942.9193

2.1 Compression Results

The results of various percentages of compression have been shown each with their attributed mean square error (MSE) relative to the ground truth, original image. The obvious trend is that as we increase compression the MSE increases. As we compress (zeroing out higher frequency components) we lose the sharpness from light to dark transition regions. This is a consequence of discarding some information containing portions of our image. It is interesting though that up to a certain percentage of compression, the reconstructed image still preserves a considerable amount of information despite how large the MSE might be. For 30% compression & even 60% compression the mean square error is quite large but the results are still quite good!

3 Wavelet Domains

In this section we explore the uses of Haar, Daubuchies 4, and Coiflet 3 wavelet bases. As an experiment, we will take a 2-level 2D wavelet decomposition of the "cameraman.tif" image in MATLAB. We want to examine the approximate image and the 6 detail coefficient images. Referring to the figures on the next page, we can see the effects of the first and second level decompositions of each image. In particular, it is almost as if introducing the detail coefficients performs edge detection for each of the images! However, we notice that as the image gets reduced more and the level increases, too much information is lost and the image is no longer able to be reconstructed. This was the common trend across all three wavelet domains so now let's examine the Fourier transform magnitudes of a standard basis element in a 256x256 matrix space (i.e. 0 elsewhere other than at the location of the standard element).

Haar Wavelets

For the Haar wavelet transform, the magnitude spectrum of its Fourier transform shows practically no variance along any of the dimensions. This implies that its Fourier transform follows a uniform distribution!

Coiflet 3 Wavelets

Next up, the Coiflet 3 wavelet transform has an interesting looking fourier domain spectrum. Judging from the result, the fourier domain magnitudes are mostly all zero around the center and taking higher values out on the edges. An observation I made about this is that it indicates sparsity. These constant spikes in the spectrum close to the center

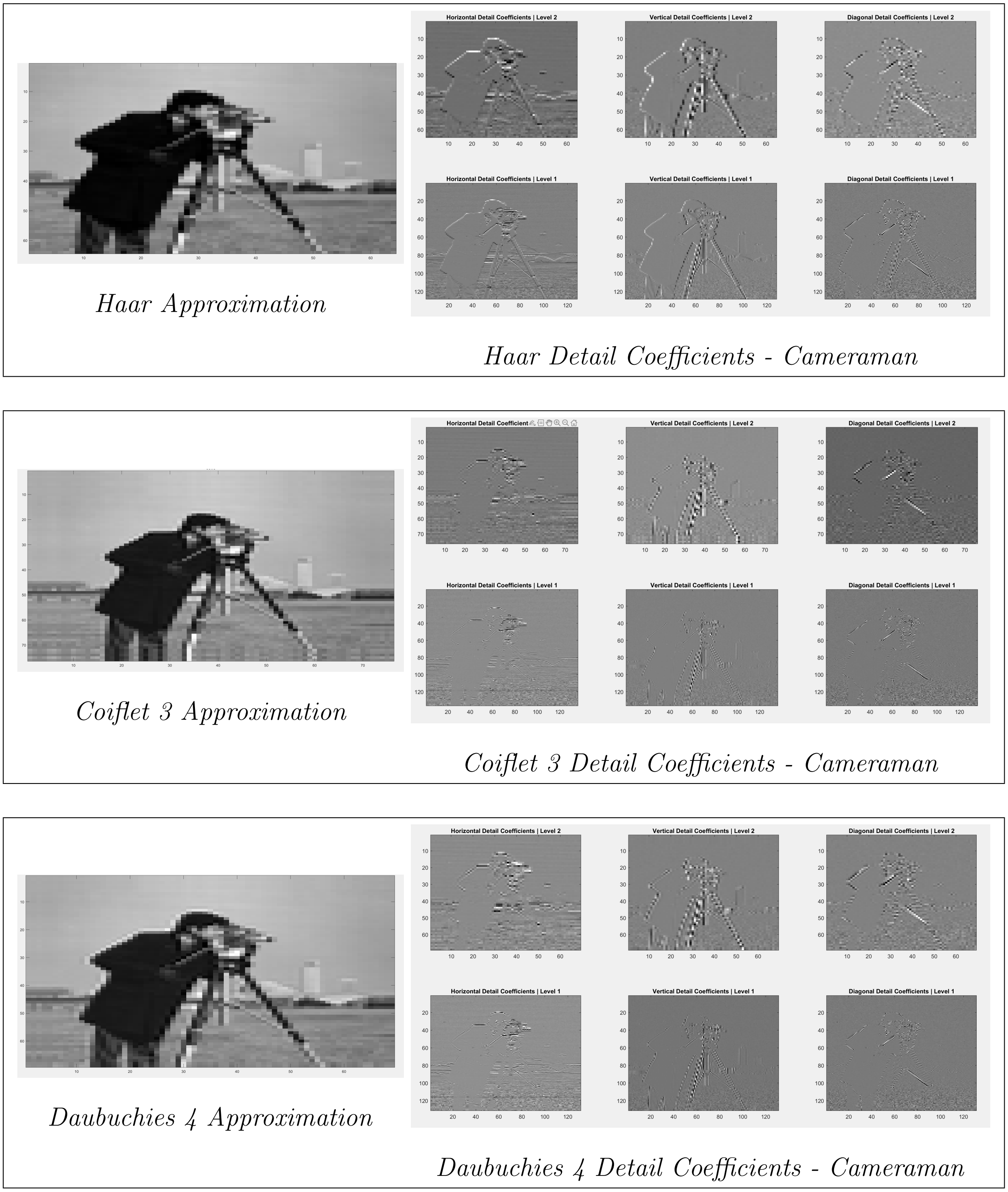

Figure 5. Decomposition of Images Into Approximation & 6 Detail Coefficients for the 3 Wavelets

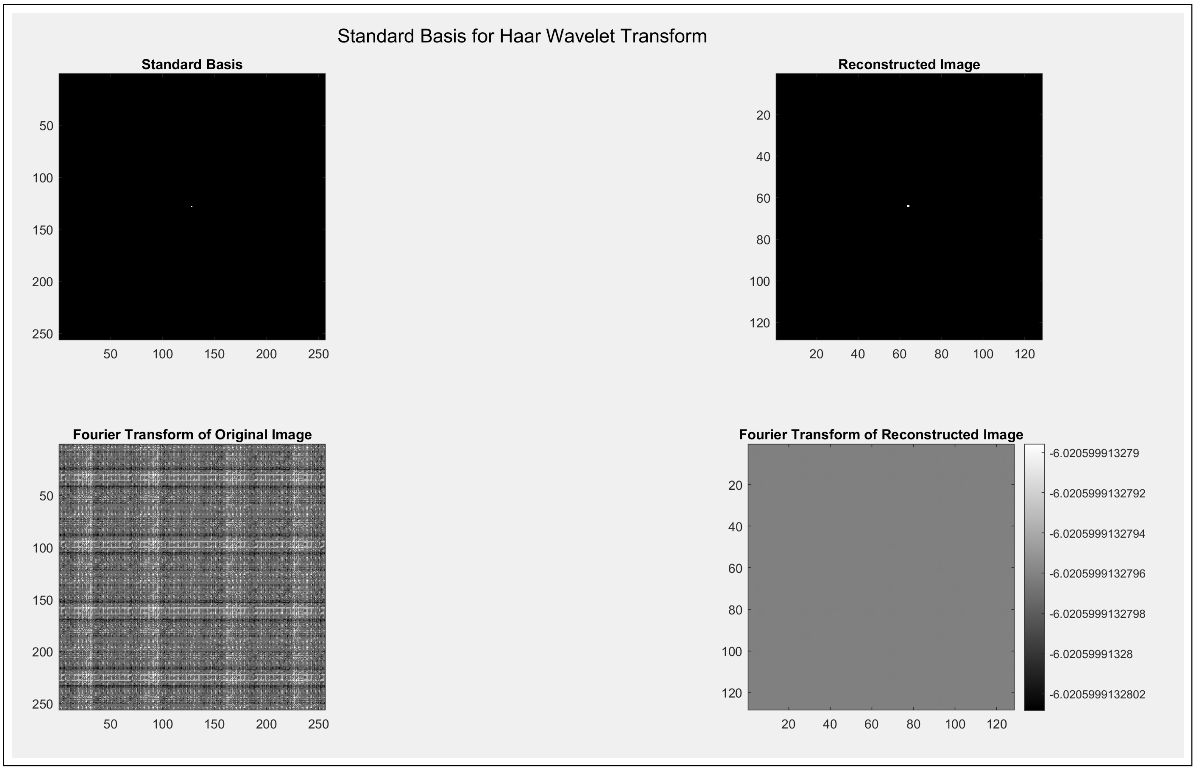
Standard Basis for Haar Wavelet Transform
Standard Basis
Reconstructed Image
Fourier Transform of Original Image
Fourier Transform of Reconstructed Image
-6.020599913279
-6.0205999132792
-6.0205999132794
-6.0205999132796
-6.0205999132798
-6.02059991328
-6.0205999132802

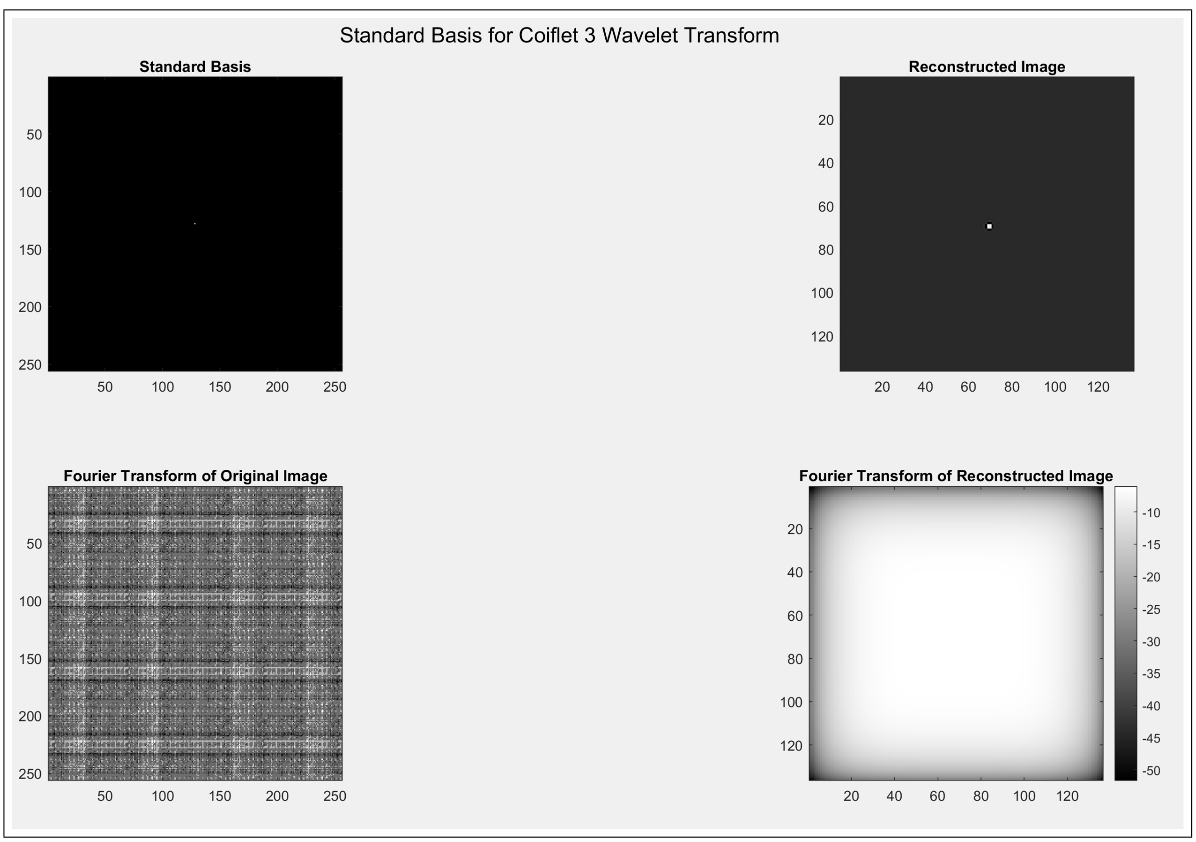
Standard Basis for Coiflet 3 Wavelet Transform
Standard Basis
Reconstructed Image
Fourier Transform of Original Image
Fourier Transform of Reconstructed Image

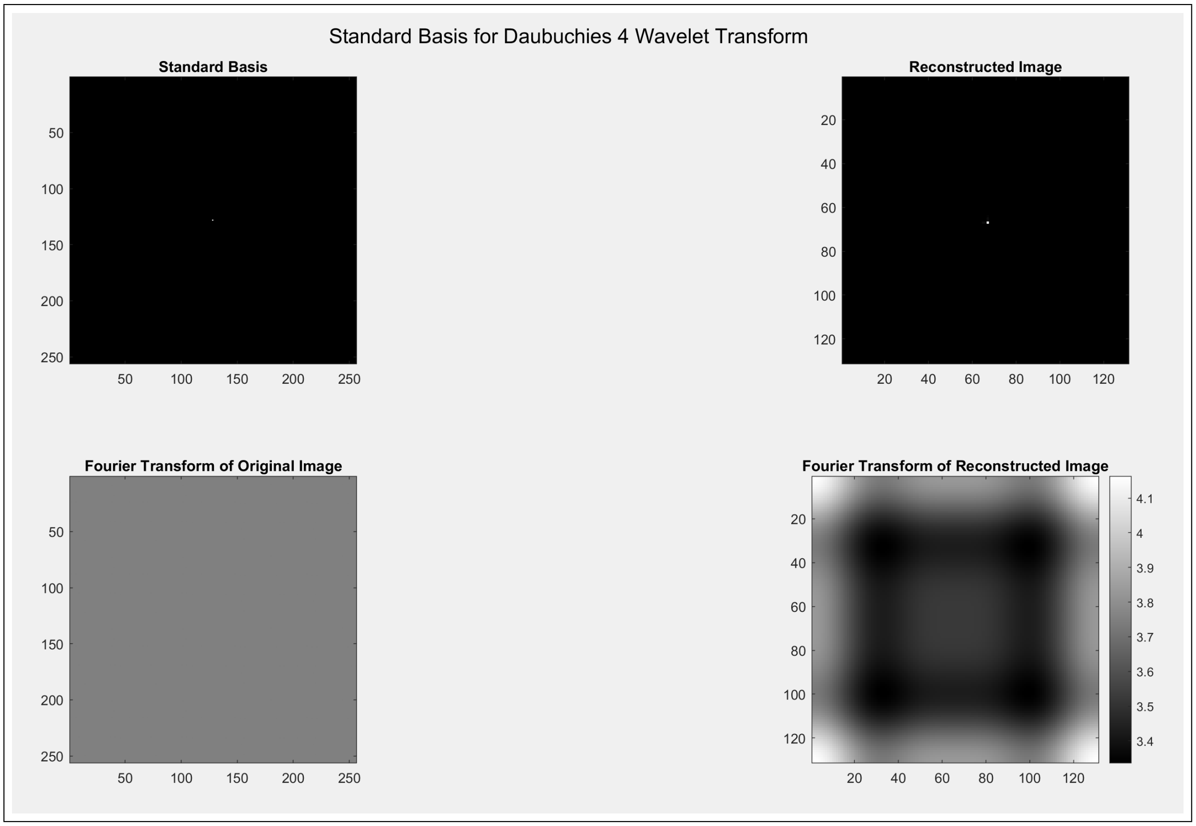

point show that most of the coefficients in this domain are very small which points to this sparse property.

Daubucheis 4 Wavelets

And finally for the Daubucheis 4 wavelets we notice once again a localization of small pixel values towards the center and larger ones as we deviate from the middle. However, this time the magnitudes are a little larger than 0 all around so I cannot say much about a sparse interpretation here.

3.1 Wavelet Decomposition of Images

In this section we can view the results of the 2 level decomposition of the guiding images in these three bases. Furthermore, we can examine the histogram of the total set of coefficients in these three bases after the 1-level, 2-level, and 3-level decompositions to determine which domain is best for compressed sensing. This is a typical approach at first to compressed sensing where the optimal domain to perform decomposition in is unknown. Because without sparsity we cannot assume this prior.

On the following page we can compare the deconstruction results for each of the three wavelet bases. On inspection I thought the Haar wavelets did the best job of encoding fine details as the deconstruction level increased each level. That is my personal analysis since at the end of the day these images need to be ready for real-world medical applications where legibility is the most important factor. For instance, even if judging from the histograms alone and you decide the best method based on which exhibits the greatest sparsity I doubt this would be the best decision to make in reality. Because at the end of the day, it is the primary objective to examine these images in order to extract qualitative information about the patient.

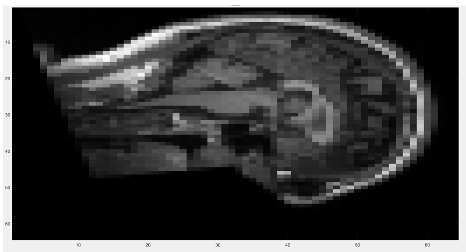

Haar Approximation

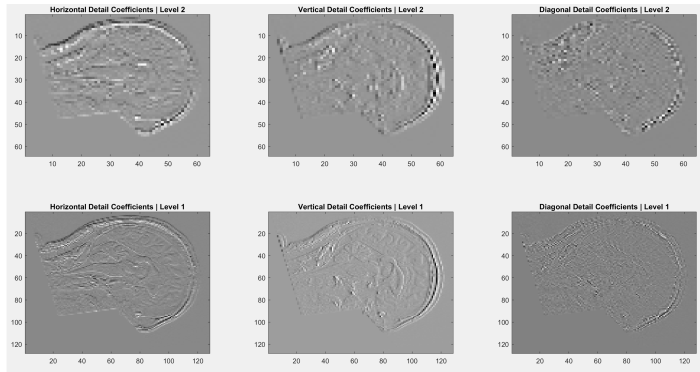

Haar Detail Coefficients - MRI Scan

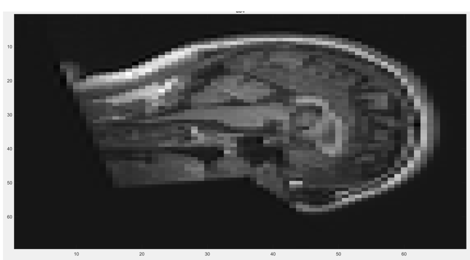

Daubucheis 4 Approximation

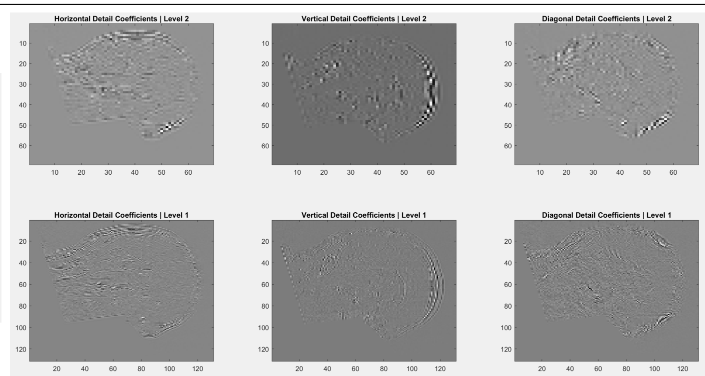

Daubucheis 4 Detail Coefficients - MRI Scan

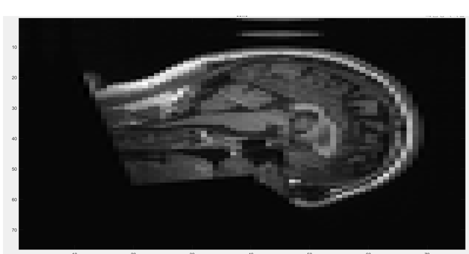

Coiflet 4 Approximation

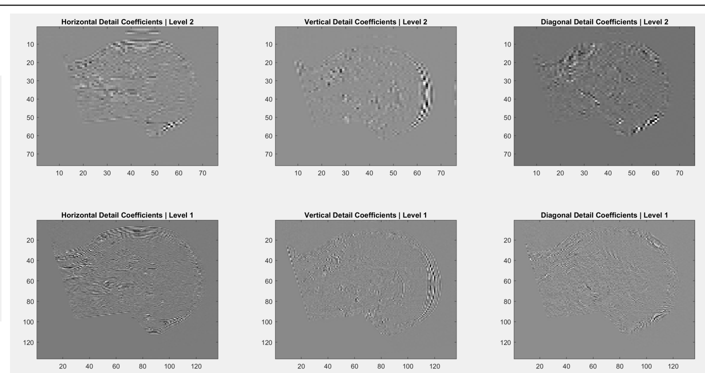

Coiflet 3 Detail Coefficients - MRI Scan

Haar Histogram

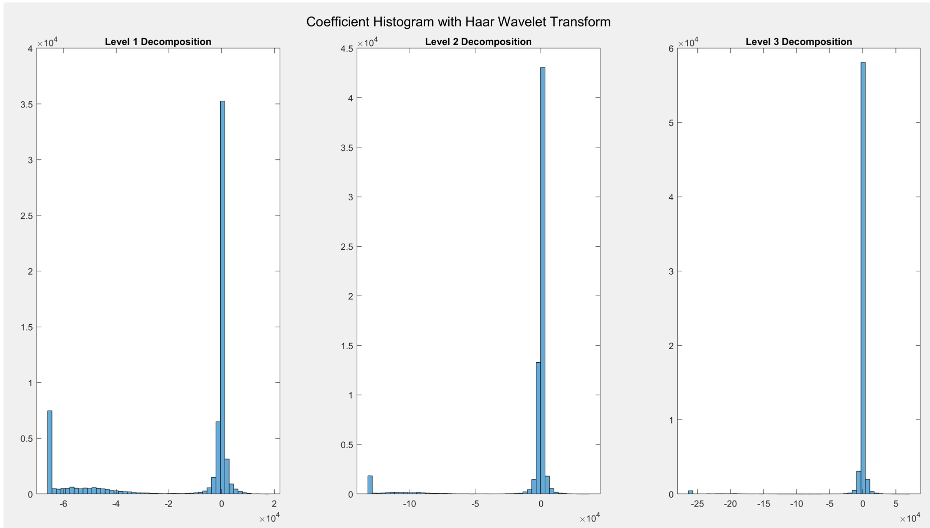

Daubucheis 4 Histogram

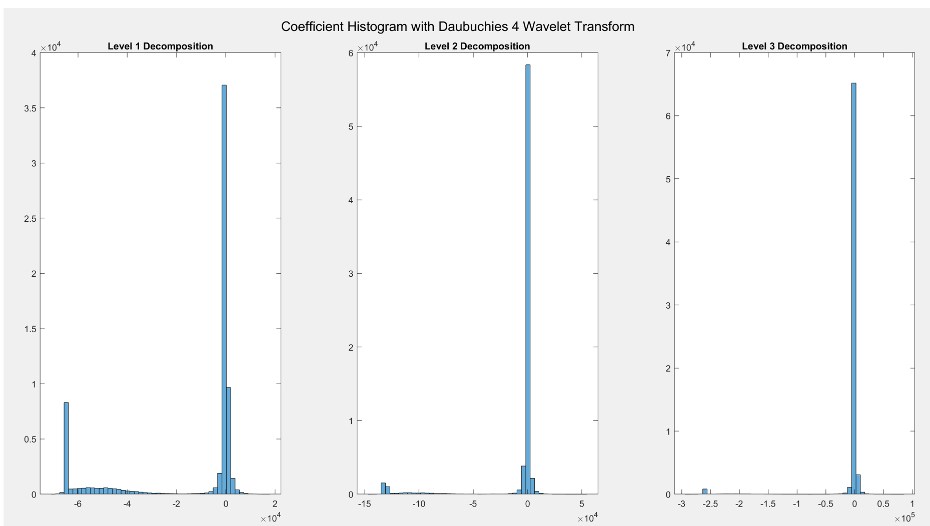

Coiflet 3 Histogram

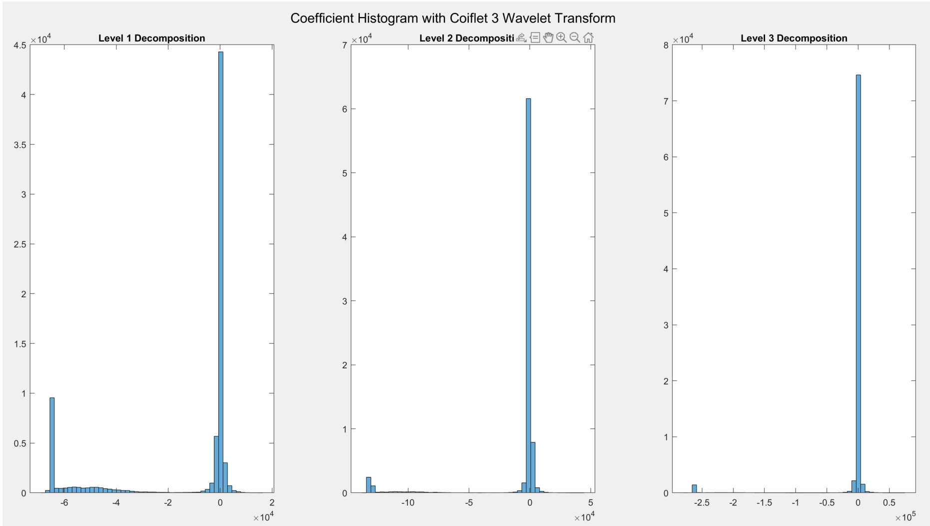

3.2 Histogram Analysis

Before moving on we can examine the histogram plots to further verify sparsity in the domain. Given the plots, we can see that there were the greatest number of occurrences of small coefficient values for the Coiflet 3 Wavelets. However, as I stated earlier, I was more pleased with the performance of the Haar wavelets from a clinical perspective, thus I am choosing this one.

3.3 Haar Wavelet Decomposition

From the reconstructed image in Figure 6 with 10% zeroed coefficients, we can see a great reconstruction! This is quite impressive because we are able to identify sparse components to throw away while maintaining good results. If this trend continues as we increase the number of zeroed coefficients, then we will have successfully decomposed the image optimally.

4 How Sparse?

Now that we have acquired what appears to be an optimal wavelet basis to use for wavelet decomposition, we want to take a look at the mean square error between the reconstructed signal and the guiding signal as a function of the percentage of coefficients zeroed out. This will indicate the (theoretical) best wavelet domain to use by examining how sparse each data set is in the context of this wavelet decomposition experiment. The ”more resilient to compression” wavelet domain will be the one that effectively sees the smallest mean square error as the percentage of samples thrown away increases.

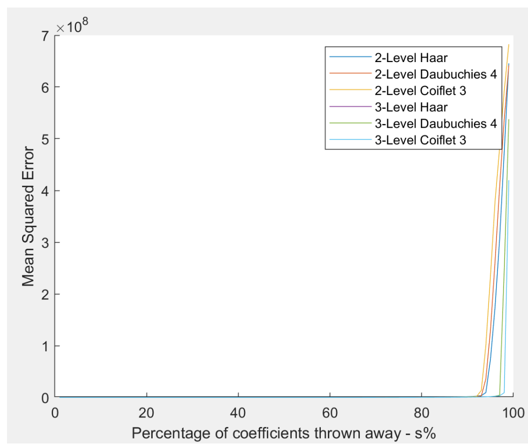

Figure 7. MSE vs s%

Analyzing Figure 7 shows that using 3-level Coiflet 3 wavelets for wavelet decomposition in this experiment preserves the most information as more and more sparse samples are zeroed out. We can also see the obvious trend in MSE as s% increases. This is

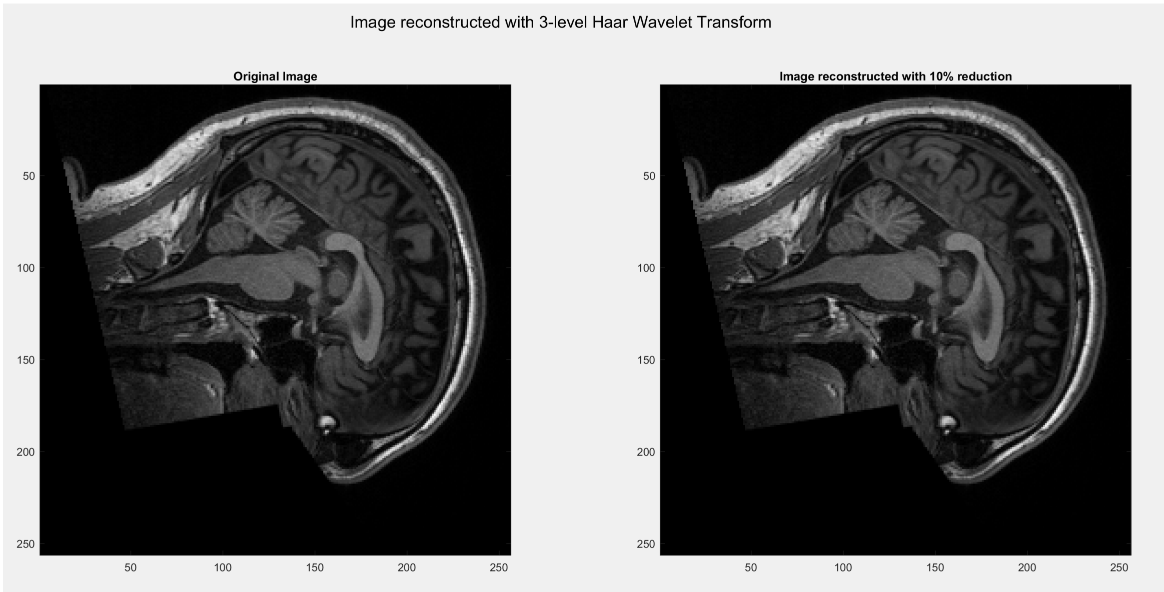

Figure 6. 10% Zeroed Coefficients - Wavelet Decomposition - Haar Wavelet

most certainly the case because if you consider the maximal case of s% = 100%, then all of our signal is thrown away which is "quantified" by an infinite mean square error. With fewer less and less information bearing coefficients, the more the reconstructed image varies compared to the guiding image.

Other distinctions that can be made regarding at what point can diminishing returns come into play? Just visually comparing the decomposed images on the following page, great feature extraction can still be maintained up to s% = 90%! Notice for instance how the white matter, grey matter, and cerebrospinal fluid regions can still be easily seen. Recall that the guiding image used in all these experiments has been from T1-weighted imaging which results in the brightest regions are white matter while the darkest regions are cerebrospinal fluid.

10% Accepted MSE Boundary

Since we have sparse data it would be reasonable to define some upper bound on the maximum acceptable MSE for a "threshold" s%. In our case, we can tolerate up to $s\% \leq 93.822$. This seems quite significant! So, for our MRI images if we choose s% up to 92% we can guarantee a MSE of less than 10% in the reconstructed image.

The real tradeoff here is of course the information contained in the reconstructed signal but what is gained is computational efficiency in these large MRI datasets. We motivated this idea in class with some examples. Overall, MRI is used for clinical application which is why reducing this time can be handy.

5 Compressed Sensing

In this final section we will explore the gradient descent algorithm that can simulate compressed sensing for MRI images by utilizing the prior of sparsity in the wavelet domain. Thus in order to proceed I will need to pick one of the wavelet domains from earlier that is sufficiently sparse. From the findings in the previous sections, we should choose the wavelet domain which exhibited the least MSE since ideally our prior would assume "total sparseness", if you will, which is obviously impossible. Therefore we will use Cloiflet 3 wavelets. Taking the ground truth to be the guiding image in the k-domain (F.T. of the guiding image) we should employ the algorithm of the form:

$$z^{k+1} = S_{\eta\vec{\lambda}}(z^k - \eta(WMW^{-1}z^n - W_y)$$

$$s.t.\ \ k = 0, 1, ...$$

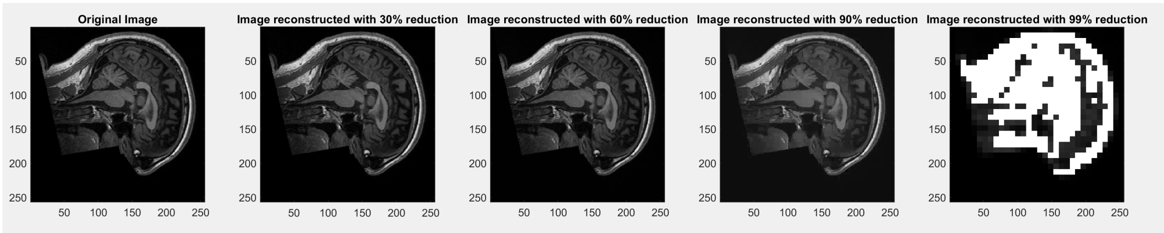

3-level Haar Wavelet Decomposition

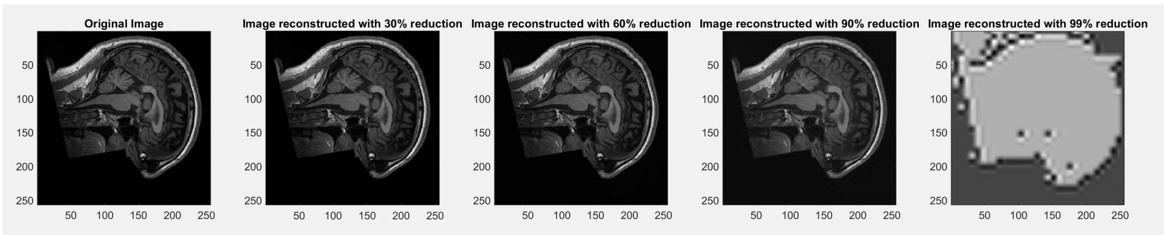

3-level Daubucheis 4 Wavelet Decomposition

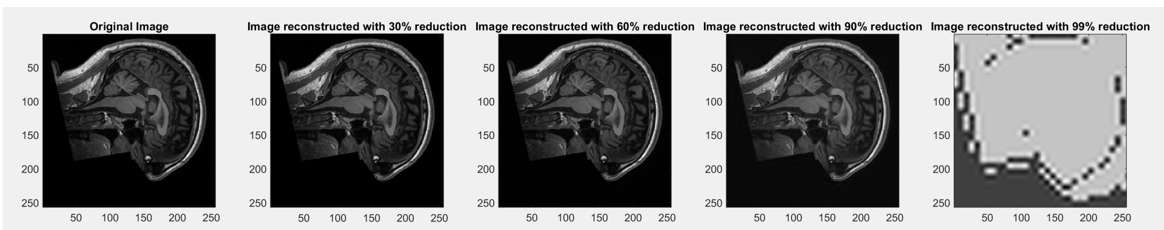

3-level Coiflet 3 Wavelet Decomposition

Where the update on z has been saved for every 10^{th} iteration so that the objective function can be plotted. Referring to the guiding image and reconstructed images comparison for compressed sensing on the next page, we can see the ability of this algorithm to reconstruct images from sparse representations.

Algorithm Analysis

Without showing other runs of this algorithm in this report (to save space) I will comment on the performance of this algorithm for different undersampling probabilities and step sizes. The first trend I noticed consisted of the trend in objective function for increase step size. As step size increase the objective function becomes less stable. The way I interpreted it is that the objective function becomes less convex as the step size increases which leads the algorithm to fall apart.

Raising and lowering the probability of undersampling had a significant effect on the reconstructed image as well. Raising this probability led to noisier reconstruction images which makes sense because there was now a higher probability that a pixel would be replaced with a zero essentially. This error compounds over time. Thus, one should suspect that the lower the probability of undersampling the better, which is true, except the way I believe is the correct way to interpret this is that with a probability of undersampling equal to zero, this effectively defeats the purpose of compressed sensing in the first place. If the goal is to undersample to beat classical Nyquist theory,

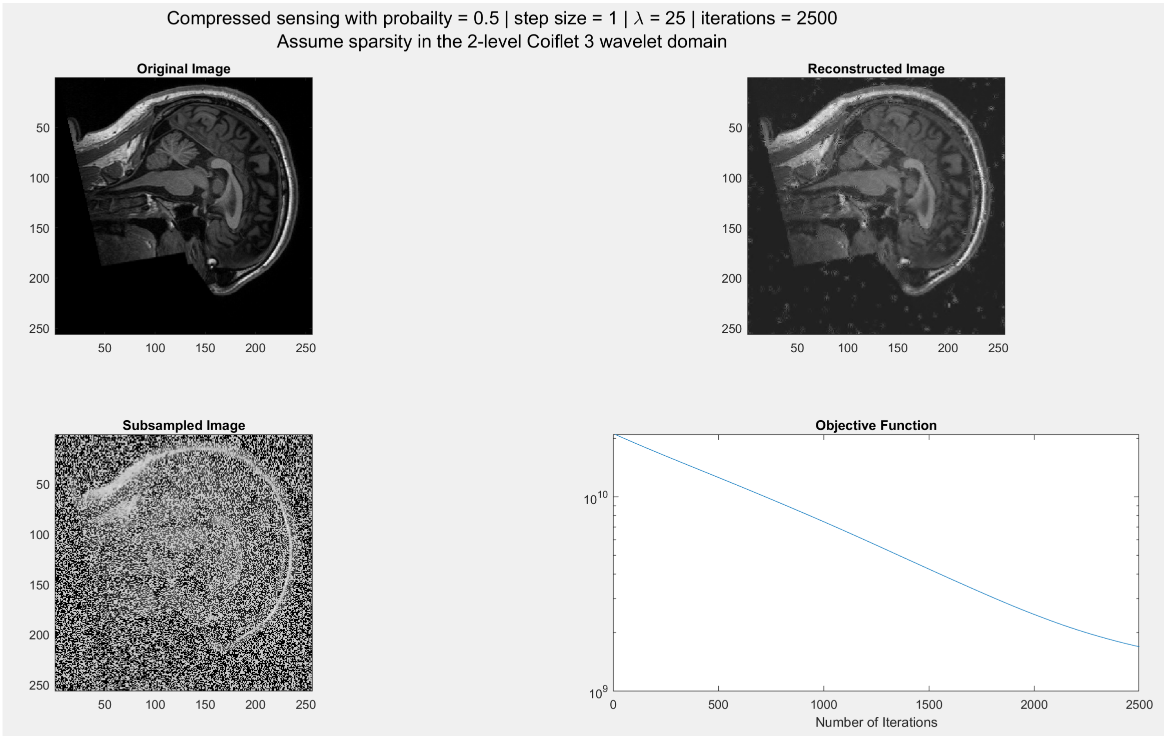

Compressed Sensing for step size = 1

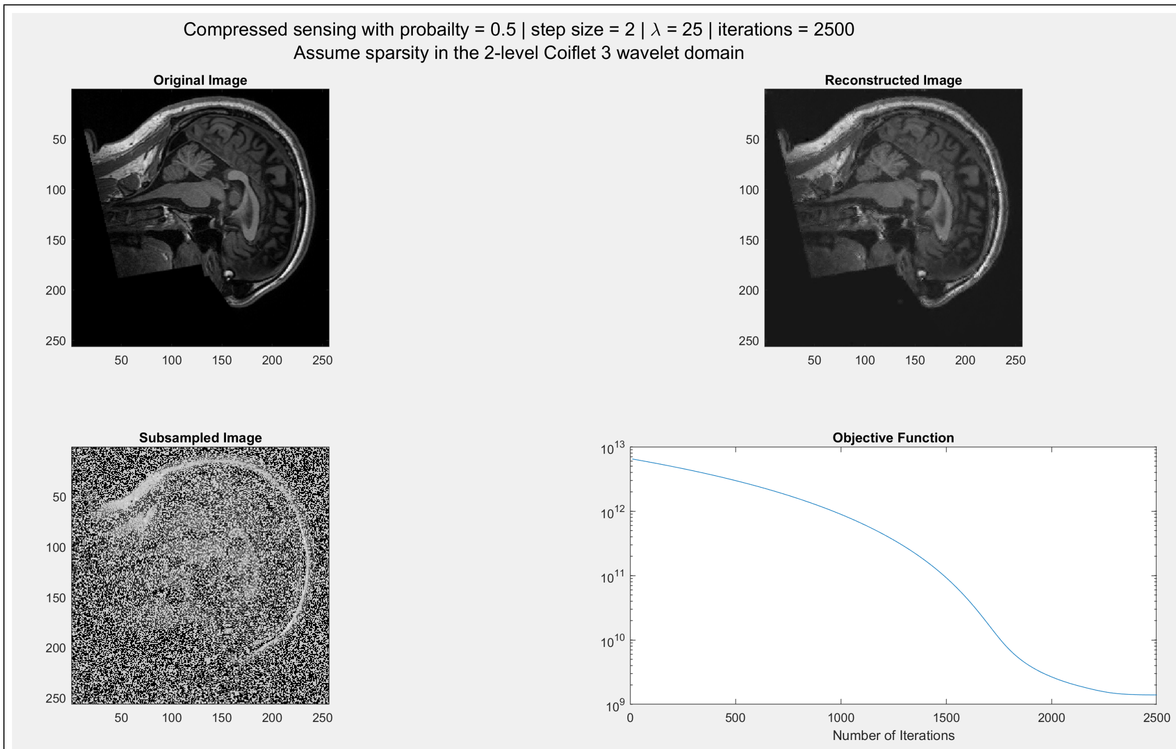

Compressed Sensing for step size = 2

then we should avoid letting the probability of undersampling from becoming too low. All this leads me to reason that the optimal probability of undersampling to use would be 0.5 so that we do not lean towards any side of this tradeoff spectrum at all. But also the notion of equiprobable probability of some quantity just sounds right to maximize some measure of "efficiency" for some stochastic process.

6 Conclusion

Throughout this project I learned more about Wavelets for image processing by exploring its applications in MRI. We built up to the idea of compressed sensing by motivating the idea of sparsity in the wavelet domain through histograms of the coefficients. When most coefficients are localized about zero we know that our domain is "sparse". From here we proved this by removing a percentage of the lowest magnitude coefficients all the way up to 99%. The results also showed that through random undersampling we can effectively process more data than predicted by Nyquist once again because of sparsity. Since there exist just a handful of information bearing coefficients we can represent the data using smaller bases consisting of these different wavelets.

And finally, after pinpointing these various results enough intuition had been built that we could proceed to defining a gradient descent algorithm to simulate compressed sensing. Through this, it was shown how the probability of undersampling is correlated with the reconstructed image, as well as a chosen step size. The objective function was plotted as well.

I personally found the results and takeaways of this project to be quite astounding in the way they just work. It is incredible how we can leverage the fact how MRI data inherently lives in a sparse domain which allows us to apply these methods of compressed sensing to significantly improve clinical applications of MRI from a computation perspective. From start to finish, this project was very satisfying when it came to learning about multiresolution and wavelets through this rigorous example of MRI. The in class lectures on MRI were also fascinating to me, during each new lesson. My reason for taking this class was to learn not only MRI (which far exceeded my expectations) but also the other medical imaging techniques used throughout the field so that I could decide if I want to pursue an engineering path in medical imaging. I definitely got all that I was looking for, thank you.